

Pore-Scale Study of Flow Rate on Colloid Attachment and Remobilization in a Saturated Micromodel

Qiulan Zhang,* A. Raoof, and S. M. Hassanizadeh

Abstract

Colloid attachment is an important retention mechanism. It is influenced by colloid size, pore size, and flow rate, among other factors. In this work, we studied colloid attachment experimentally under various flow rates, as well as colloid release in response to a rapid change of flow rate. Colloid transport experiments under saturated conditions and with different flow rates were conducted in a physical micromodel. The micromodel was made of polydimethylsiloxane (PDMS), which is a hydrophobic polymer. Colloids were hydrophilic fluorescent carboxylate-modified polystyrene latex microspheres with a mean diameter of 300 nm. We could directly observe the movement of colloids within the pores using a confocal microscope. We also obtained concentration breakthrough curves by measuring the fluorescence intensity at the outlet of the micromodel. In addition, our experiments were simulated using a pore-network modeling, PoreFlow, based on the pore structure of the micromodel. Local colloid concentrations were calculated by solving local mass balance equations for all network elements and then averaging resulting concentrations over the whole micromodel. The measured breakthrough curves were successfully simulated using PoreFlow. Observed and calculated breakthrough curves showed that colloid attachment rate was smaller for larger flow rate. Temporally enhance colloid release (remobilization of attached colloids) was observed when the flow rate was increased by a factor of 10. But no colloid remobilization was observed when the flow rate decreased by a factor of 10.

Core Ideas

- Colloid remobilization in response to transients in flow rate was visualized.
- Pore-network modeling was used to model concentration breakthrough curves.
- At larger flow rate, less attachment was observed.

COLLOID DEPOSITION in saturated porous media is commonly described using colloid filtration theory, developed initially by Yao et al. (1971). It assumes that the colloid attachment rate coefficient is controlled by three mechanisms: Brownian diffusion, interception, and sedimentation. Colloid filtration theory successfully predicts colloid deposition under favorable chemical conditions when no Derjaguin–Landau–Verwey–Overbeek (DLVO) energy barriers are present. There are three major assumptions inherent to the colloid filtration theory: (i) colloid and the surface collector surfaces are both perfectly smooth, (ii) effects of hydrodynamic forces are negligible, and (iii) colloids are small enough so that straining effects are not significant. However, the surface of natural colloids and collectors always contain some roughness (Suresh and Walz, 1996). Discrepancies of colloid attachment–detachment between theoretical predictions and experimental results are believed to result mainly from surface roughness (Suresh and Walz, 1996; Hoek et al., 2003; Hoek and Agarwal, 2006) and surface charge heterogeneity (Bradford and Torkzaban, 2013). Johnson et al. (2011) also argued that surface charge heterogeneity and surface roughness may result in enhanced colloid attachment under unfavorable conditions. Indeed, colloid deposition has been found to increase on rough surfaces in studies using atomic force microscopy (Shellenberger and Logan, 2002; Chen et al., 2010) and with digital bright field microscopy (Morales et al., 2009).

Another mechanism for colloid retention is reported to be straining in saturated porous media. Straining was regarded as the dominant retention mechanism under unfavorable attachment conditions, for example, when DLVO energy barriers are present (Bradford et al., 2002, 2003, 2005; Li and Johnson, 2005; Li et al., 2006; Xu et al., 2006, 2008; Johnson et al., 2007; Shen et al., 2008; Du et al., 2013).

Colloid retention was also reported to be affected by flow velocity in saturated porous media (Bradford et al., 2007, 2011; Johnson et al., 2007; Du et al., 2013). Researchers found that at higher flow velocity, colloid straining was less in porous media under unfavorable chemical conditions. Colloid attachment–detachment is also known to be affected by forces and torques

Copyright © 2015 American Society of Agronomy, Crop Science Society of America, and Soil Science Society of America. 5585 Guilford Rd., Madison, WI 53711 USA. All rights reserved.

J. Environ. Qual. 44:1376–1383 (2015)

doi:10.2134/jeq2015.01.0058

Supplemental material is available online for this article.

Received 31 Jan. 2015.

Accepted 29 July 2015.

*Corresponding author (qlzhang919@cugb.edu.cn).

Q. Zhang, Faculty of Water Resources and Environment, China Univ. of Geosciences, Chengfu Rd. 20, Beijing, 100083, P.R. China; A. Raoof and S.M. Hassanizadeh, Earth Sciences Dep., Utrecht Univ., Budapestlaan 4, 3584 CD Utrecht, the Netherlands. S.M. Hassanizadeh, Soil and Groundwater Systems, Deltare, the Netherlands. Assigned to Technical Editor Scott Bradford.

Abbreviations: DI, deionized; DLVO, Derjaguin–Landau–Verwey–Overbeek; PDMS, polydimethylsiloxane; PNM, pore-network model.

that act on colloids (Cushing and Lawler, 1998; Torkzaban et al., 2007). Under favorable conditions, the adhesive force due to DLVO interactions dominates and therefore results in colloid retention (Torkzaban et al., 2007; Bradford et al., 2009). However, under unfavorable conditions, hydrodynamic shear may not be negligible (O'Neill, 1968; Weisbrod et al., 2002). The induced shear force is opposed by the adhesive force due to DLVO interactions (Bergendahl and Grasso, 1998; Cushing and Lawler, 1998; Torkzaban et al., 2007; Bradford and Torkzaban, 2008).

Some researchers have studied the combined effect of DLVO force and hydrodynamic force on colloid attachment to and detachment from a collector surface (Cleaver and Yates, 1973; Sharma et al., 1992; Bergendahl and Grasso, 1998; Burdick et al., 2005; Seetha et al., 2014). Bergendahl and Grasso (1998) illustrated how polystyrene microspheres attached to glass beads in a packed column could be detached by hydrodynamic shear force, depending on the flow velocity and the magnitude of the DLVO interaction forces. Johnson et al. (2007) demonstrated that large colloids may experience a larger hydrodynamic shear force at a given flow rate and solution chemistry.

As a surrogate for experimental work, one can use pore-scale models to provide detailed information on transport processes at the microscopic (pore) scale. Moreover, using pore-scale modeling, it is possible to develop macroscale relationships for attachment–detachment rates. One widely used approach is the use of a pore-network model (PNM). Compared with other pore-scale modeling approaches, PNMs allow simulation of transport processes over larger domain sizes, thus making it possible to upscale processes from the pore scale to the macroscale (see, e.g., Raoof et al., 2013). Pore-network modeling has been extensively used to obtain pore-scale information (Nsir and Schäfer, 2010; Bodla et al., 2010; Varloteaux et al., 2012; Raoof and Hassanizadeh, 2012). For example, PNM approaches have been used in the upscaling of reactive–adsorptive transport (Acharya et al., 2005; Raoof et al., 2010; Kohne et al., 2011).

The effect of flow rate on colloid attachment under steady-state saturated conditions has been studied by a number of researchers. But the role of transients in flow rate in colloid remobilization is not yet well understood. The aim of this study was to examine the effect of flow rate on colloid retention and transients in flow rate on colloid remobilization in saturated porous media at the pore scale. Pore-scale visualization experiments and concentration breakthrough measurements were conducted at various flow velocities in a polydimethylsiloxane (PDMS) micromodel. We also used pore-network modeling, PoreFlow (Raoof et al., 2013), to obtain more quantitative pore-scale information on the dependence of the attachment–detachment coefficient on the flow rate. We further provided comparisons of the pore-network simulation results to experimental data.

Materials and Methods

Micromodel Experiments

The PDMS micromodel used in our experiments contained 98 pore bodies (large pores) connected by 217 pore throats (smaller pores). The flow network of the micromodel was designed based on Delaunay triangulation (see Karadimitriou et al., 2012); it is shown in Fig. 1. The flow network covered an area of 1 mm by

10 mm, with a mean pore size of 30 μm and a uniform depth of 30 μm . The properties of the micromodel are shown in Table 1. The PDMS micromodel was treated by a silanization process (see Karadimitriou, 2013, Chapter 5). In this process, a solution of silane in 96% pure ethanol was used to make the micromodels uniformly and stably hydrophobic. Fluorescent carboxylate-modified polystyrene microspheres with a mean diameter of 300 nm (Polysciences Inc. GmbH) and a particle density of 1.055 g/cm³ (reported by the manufacturer) were acquired (Polysciences Inc. GmbH) and used as model colloids. The particles were hydrophilic and had negatively charged surfaces. The colloid suspension was diluted by dispersing it in deionized (DI) water to reach a final concentration of around 5.8×10^{10} particles per liter. Before the dilution, the suspension was sonicated in an ultrasonic bath for 2 min to ensure uniform particle distribution. The stock solution was also sonicated before using it in experiments. The pH of the stock solution was monitored and kept between 6.8 and 7.0 during the experiments. Also, the value of ionic strength was kept constant at 1.2×10^{-3} mM.

Details of the experimental set-up can be found in Zhang et al. (2013). A schematic representation of the setup is shown in Fig. 2. Using a confocal laser microscope, images were acquired of the movement of colloids in the micromodel. The microscope was also used to measure the colloid concentration breakthrough curves in the outlet channel, as described below. A dual-direction syringe pump was used to control the flow rates of the liquid and colloid suspension via a three-way valve.

Two types of experiments were performed: steady-state and transient. The steady-state experiments were conducted in two stages. In the *first stage*, a fully saturated steady-state flow of water with no colloids was established. To do this, the micromodel was placed vertically and then flushed with carbon dioxide for a few minutes to expel the air. The micromodel was then positioned horizontally on the stage of the confocal microscope and connected to the injection tubes. Next, DI water was introduced into the micromodel at a specified constant flow rate to displace and dissolve the carbon dioxide, until a fully saturated steady-state flow of water was established. We performed three sets of experiments at three different flow rates: 50, 250, and 500 nL/min. These are denoted by q , $5q$, and $10q$, respectively.

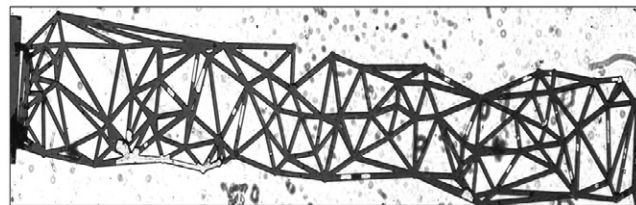


Fig. 1. The micromodel flow network.

Table 1. Properties of the pore network (the micromodel).

Parameters	Values
Number of pore bodies	98
Number of pore throats	217
Mean pore body size (diameter)	30 μm
Depth of the flow network	30 μm
Area of the flow network	1 mm \times 10 mm
Porosity	0.39

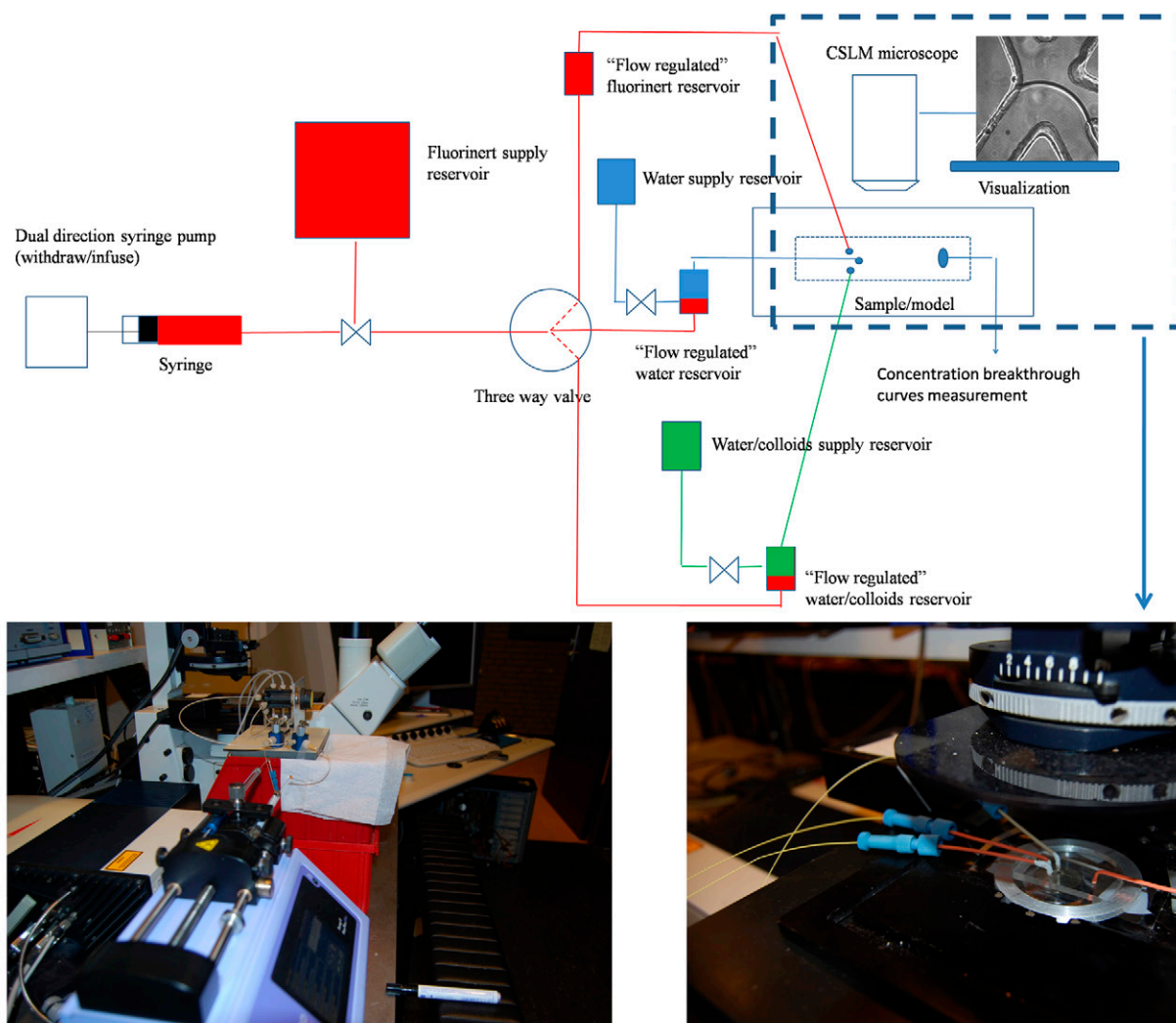


Fig. 2. Schematic representation of the experimental set-up.

In the *second stage*, still under steady-state flow conditions and keeping the flow rate constant, a particle suspension was injected for 20 min. This was followed by the injection of colloid-free DI water for 25 min, again without changing the flow rate. Thus, the second stage of each experiment (i.e., colloid transport during steady-state flow) lasted 45 min.

We also performed transient flow experiments. For these experiments, a third stage was added to the above-mentioned procedure. At the start of stage three, the flow rate was abruptly changed by a factor of 5 or 10. Four series of transient flow rate experiments were conducted: flow rate increased from 250 nL/min to 2.5 μ L/min, from 50 nL/min to 250 nL/min, from 250 nL/min to 1.25 μ L/min, and decreased from 500 nL/min to 50 nL/min.

Theoretical Calculation of Interaction Energies/Forces

The interaction energies among colloids and between colloids and the PDMS surface were estimated using the classic DLVO theory (Derjaguin and Landau, 1941; Verwey and Overbeek, 1948). The van der Waals attraction was calculated based on an expression proposed by Gregory (1981), whereas the electrical double layer interaction for a sphere with a surface was estimated using an equation presented by Norde and Lyklema (1989).

The total interaction energy (ΔG_{tot}) can be expressed as follows (Gregory, 1981):

$$\Delta G_{\text{tot}} = 64\pi\epsilon R \left(\frac{kT}{ve} \right)^2 \gamma_1 \gamma_2 \exp(-\kappa b) - \frac{A_{123}R}{6b} \left[1 - \frac{5.32b}{\lambda_0} \ln \left(1 + \frac{\lambda_0}{5.32b} \right) \right] \quad [1]$$

where R is the radius of the particle; ϵ is the dielectric permittivity of the liquid (in this case, 80.1 for DI water); k is the Boltzmann constant; T is absolute temperature; v is the ion valence; e is the electron charge; $\gamma_i = \tanh[ve\psi_{0,i}/(4kT)]$; κ is the Debye-Hückel reciprocal length; b is the separation distance; A_{123} is the Hamaker constant; and λ_0 is a characteristic length of 100 nm. The two terms in this equation are due to electrostatic and van der Waals interaction energies, respectively.

The calculated DLVO interaction energy profile between the colloid (in DI water) and the PDMS surface is shown in Fig. 3. For these calculations, the zeta potential of polystyrene microspheres was taken to be -36.6 mV (measured using a Zetasizer, Malvern Instruments), and the zeta potential of the PDMS surface was taken to be -80 mV (Sze et al., 2003). A value of 3.9×10^{-21} J was used for the Hamaker constant of the polystyrene-

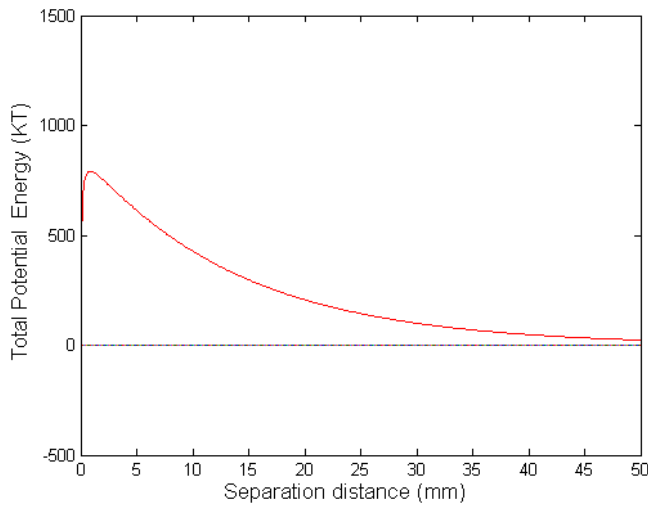


Fig. 3. Calculated Derjaguin–Landau–Verwey–Overbeek energy profile for the interaction between colloid with polydimethylsiloxane surface.

water–PDMS system, as calculated in other studies (Israelachvili, 1992; Bradford and Torkzaban, 2008). As can be seen in Fig. 3, a significant energy barrier exists between the colloid and the PDMS surface, while a secondary minimum is absent, which means that colloid attachment to the PDMS surface is highly improbable in DI water. One should note that we did not consider any surface charge heterogeneity and surface roughness in our calculations. Hydrophobic interactions are also neglected in the calculations.

On a rough surface, a colloid may experience a friction force against movement. A schematic of forces acting on a colloid, with radius R , attached to a rough PDMS solid surface in moving water is shown in Fig. 4. The forces shown in the figure are Van der Waals force (F_{vdw}), electrostatic force (F_{el}), drag force (F_D), friction force (F_{fric}), hydrodynamic torque (T_{hydro}) and resisting torque (T_{resist}).

The total DLVO force is given by

$$F_{DLVO} = \frac{d}{dh}(\Delta G_{tot}) \quad [2]$$

The drag force can be expressed as follows (Goldman et al., 1967; O'Neill, 1968):

$$F_D = 10.205\pi\mu\left(\frac{\partial V}{\partial R}\right)R^2 \quad [3]$$

where μ is the water dynamic viscosity and $\partial V/\partial R$ is the shear rate to be calculated at a distance of R from the surface.

The friction force is given by

$$F_{fric} = \mu_f F_{DLVO} \quad [4]$$

where μ_f is the static friction coefficient.

These three forces also may exert a nonzero torque on the colloid even if their own resultant is zero. The adhesive torque for colloids is expressed as

$$T_{resist} = F_{DLVO} l_x \quad [5]$$

The hydrodynamic torque caused by a drag force is given as (Goldman et al., 1967; O'Neill, 1968):

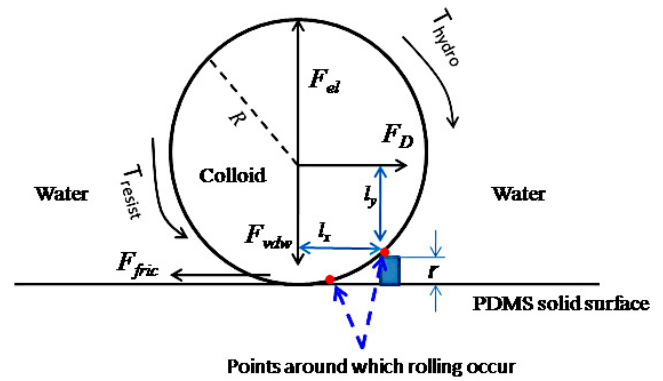


Fig. 4. Schematic of forces acting on an adhering colloid in moving water.

$$T_{hydro} = F_D l_y \quad [6]$$

where l_x and l_y are the lever arms of the DLVO and drag forces, respectively. If the roughness height is denoted by r , the lever arms are given by the following:

$$l_y = R - r$$

$$l_x = \sqrt{R^2 - l_y^2} = \sqrt{2rR - r^2}$$

Pore-Network Modeling

Using pore-network modeling, fluid flow as well as flux of colloids and their adsorbed mass can be calculated at the scale of individual pores. We constructed a two-dimensional PNM of our micromodel, using PoreFlow (Raoof et al., 2010). The flow and transport formulations can be found in Supplemental Material 1 (Appendix A).

Results

Effect of Flow Rate on Colloid Attachment

Figure 5 presents the results of colloid concentration breakthrough curves measured and simulated at the outlet reservoir of the PDMS micromodel at three different flow rates. As can be seen, when the flow rate was q , the normalized effluent concentration reached a maximum of ~ 0.68 . When the flow rate was increased five times (to $5q$), the maximum concentration went up to ~ 0.8 . At a flow rate of $10q$, even less attachment was observed, as a maximum concentration of ~ 0.95 was reached. This reduction in colloid removal at higher flow rates is at odds with the colloid filtration theory, according to which the attachment coefficient is proportional to $v^{1/3}$. According to colloid filtration theory, attachment should be larger at higher velocities. That may be the case, but we know that is partially because the drag force increases with the flow rate, as can be seen from Eq. [3] and Eq. [4], whereas the adhesive force remains constant. This means that the colloid detachment coefficient will be larger at higher flow rates, such that the net effect of higher flow rates is an increase in removal rates of colloids.

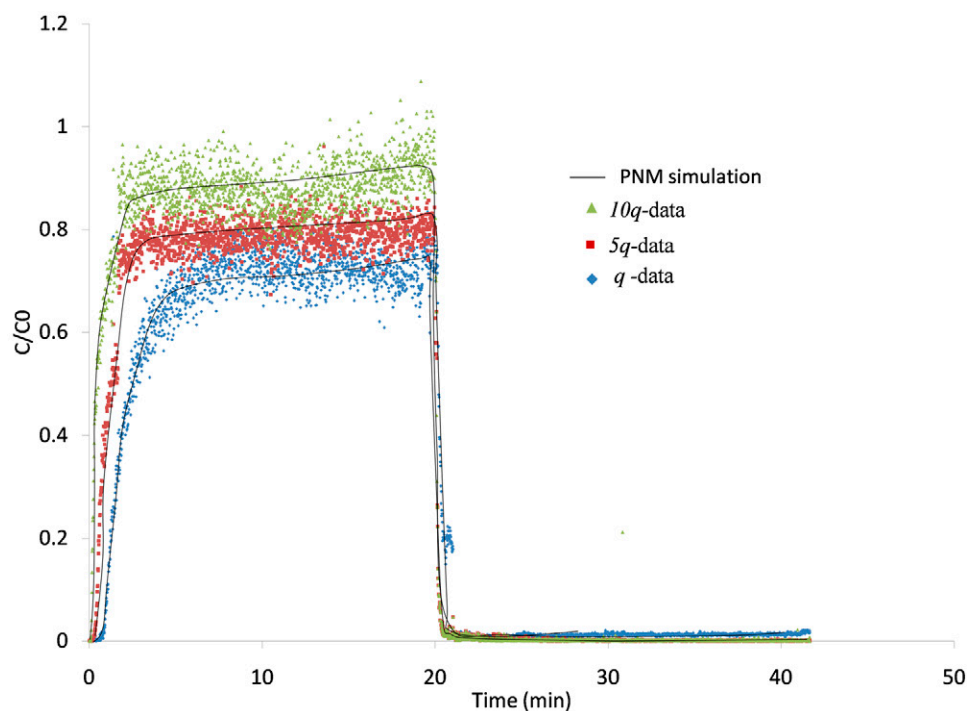


Fig. 5. Measured and simulated effluent concentration (C) breakthrough curves of colloid transported at different flow rates (q , $5q$, and $10q$). PNM, pore-network model.

Effect of Rapid Flow Rate Change on Colloid Remobilization

As explained earlier, we did experiments in which the flow rate was abruptly changed at the end of stage 2. In experiments in which the flow rate increased by a factor of 10 (from 250 nL/min to 2.5 μ L/min), we observed a clear remobilization of attached colloids. This is seen as a spike in the breakthrough curve in Fig. 6. Based on mass balance calculations, $\sim 11.5\%$ of the remaining colloids was remobilized. In experiments in which the flow rate increased by a factor of five (from 500 nL/min to 2.5 μ L/min), very little remobilization of attached colloids occurred (as can be seen in Fig. 6). In a new transient experiment, at the end of stage 3, we also conducted an experiment in which the flow rate was decreased rapidly from $10q$ to q . We did not observe a remobilization of colloids.

Real-time images of colloid remobilization during the rapid increase of flow rate can be found in Supplemental Material 2 (video). In the video, the change in the flow rate required a time period of 10 s. The video shows that after the rapid increase in the flow rate, some of the colloids that were attached to the PDMS surface in the upright pore throats were released, but some of them reattached downstream during their transport.

Three processes are involved when colloids are detached from the solid surface: sliding, lifting, and rolling. Previous studies have shown that rolling is the main mechanism for colloid detachment (Sharma et al., 1992; Burdick et al., 2001). We earlier used Fig. 3 to illustrate that colloid behavior is determined by force balance and torque balance. Only when the hydrodynamic torque overcomes the resisting torque can rolling occur. Inspection of Eq. [1–6] shows that an increase in the flow rate leads to an increase in the drag force and the hydrodynamic torque. Thus, a stably attached colloid can then be released.

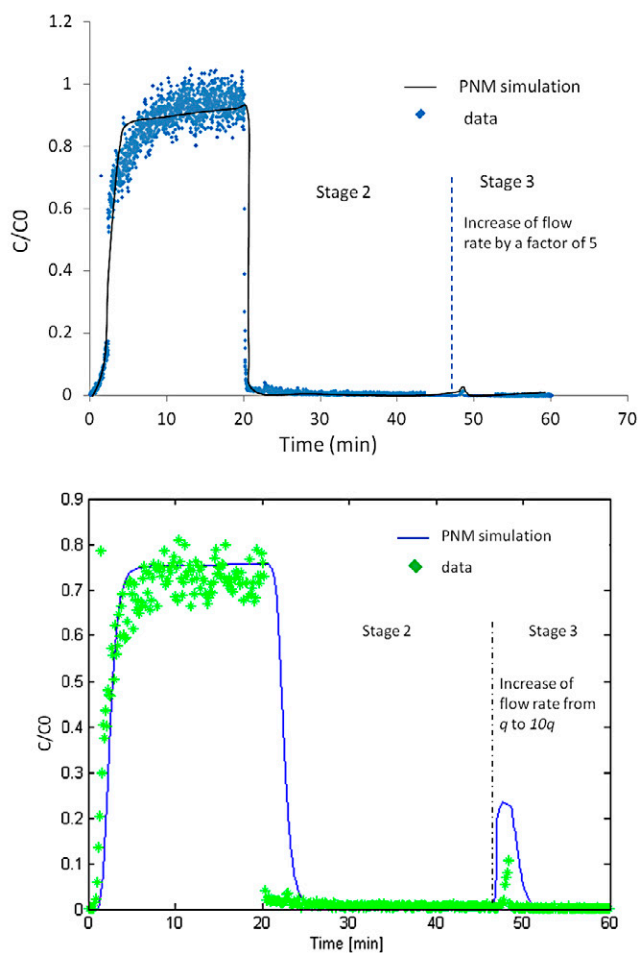


Fig. 6. Measured and simulated concentration breakthrough curves under transients in flow rate at the outlet reservoir of the micromodel during transient experiments. The top graph is for the increase of flow rate by a factor of 5, the bottom one by a factor of 10.

Discussion

The profile of the interaction energy between a colloid and the PDMS surface (see Fig. 3) shows a repulsive energy barrier. Thus, no attachment of colloids should have occurred. However, in those calculations, we did not consider surface roughness. We did some scanning electron microscope and atomic force microscope measurements of the surface roughness of the PDMS micromodel before and after silanization. It was found to be around 50 nm after saline, which is significant relative to the size of the colloids used (300 nm diam.). The theory of Bradford and Torkzaban (2013) states that nanoscale roughness can alter the energy barrier to allow primary minimum interactions, decreasing the magnitude of the secondary minimum and creating a finite depth of the primary minimum. As explained above (see Fig. 4), surface roughness may produce forces that resist the sliding or rolling of colloids along the PDMS surface. These forces then oppose the hydrodynamic forces, and the microscopic roughness alters the lever arms associated with the applied hydrodynamic and resisting adhesive torques. In addition, based on the results of Bradford and Torkzaban (2013), a colloid may be immobilized in the presence of fluid flow due to nanoscale heterogeneity on adhesive torques. Moreover, the surface roughness may locally decrease the flow velocity near the wall, which reduces the hydrodynamic force and Brownian motion, thus causing more attachment to occur. The third explanation is that colloid immobilization adjacent to macroscopic roughness locations shares many similarities to grain–grain contact points and may be viewed as a type of straining process (Bradford and Torkzaban, 2013).

Another mechanism that may cause the retention of colloids is straining at very small pore openings and around points of contact of solid surfaces. Du et al. (2013) demonstrated theoretically that retention of colloids in DI water is mainly due to colloids straining at stagnant zone where grain–grain contacts exist. Other studies (e.g., Bradford and Bettahar, 2006; Bradford et al., 2009; Torkzaban et al., 2010) also showed that the retained colloids at lower ionic strength (<0.001 M) were mainly strained at grain–grain junctions, which suggests that the main retention mechanism at low ionic strength is straining. However, in our micromodel, we did not have any grain–grain contact zones. This is because the pore throats in our micromodel had parallel walls (as seen in the video in Supplemental Material 2). Hence, straining could not occur in our micromodel. Thus, our observation is similar to Johnson and Tong (2006) and Johnson et al. (2010, 2011) in that the main attachment mechanism in the micromodel was due to surface roughness.

Our findings disagreed with Shen et al. (2012), who reported that the rough asperity (which is ubiquitous) on collector surfaces provides a tangential attraction force that can prevent colloids from being swept away by hydrodynamic shear. However, we note that in their case, the solution ionic strength was much larger than 0.01 M.

The PNM PoreFlow was used to simulate colloid breakthrough curves. In doing so, we chose values of pore-scale detachment coefficients for each pore, $k_{det,ij}$, and distribution coefficient, $K_{d,ij}$, which are defined in Supplemental Material 1 (Appendix A), to fit the breakthrough curves as closely as possible. We found different values of $k_{det,ij}$ and $K_{d,ij}$ for different flow rates. In the

simulation, the formula $k_{det,ij} = 0.0002 + 0.0009 \cdot v + 0.001 \cdot v^2$ and $K_{d,ij} = 3 \cdot R \cdot (109.17 + 0.9786 \cdot v - 0.0085 \cdot v^2)$ was used, where R is the radius of the pore and v is the flow rate. Results are shown in Fig. 7. The measured and simulated breakthrough curves are shown in Fig. 5 and Fig. 6. Generally good agreement was obtained between the measurements and the simulations. This provides confidence that our pore-network modeling approach can be used to model the flow rate effect on colloid transport and remobilization. Further work is needed to develop relationships for macroscale attachment and detachment rate coefficients as a function of flow rate.

Conclusions

In this study, microscopic colloid transport experiments under saturated conditions and with different flow rates were conducted in a physical micromodel. The movement of colloids inside the micromodel was visualized by means of a confocal microscope. Results demonstrate that flow rate affects colloid attachment processes. Transients in flow rates cause colloid remobilization only when the flow rate increased by a factor of 10; no clear remobilization was observed when the flow rate increased by a factor of 5. Analysis of forces and model results show that only when the hydrodynamic forces and torque overcome the resisting forces and torques does remobilization occur. The experimental results could be successfully simulated using

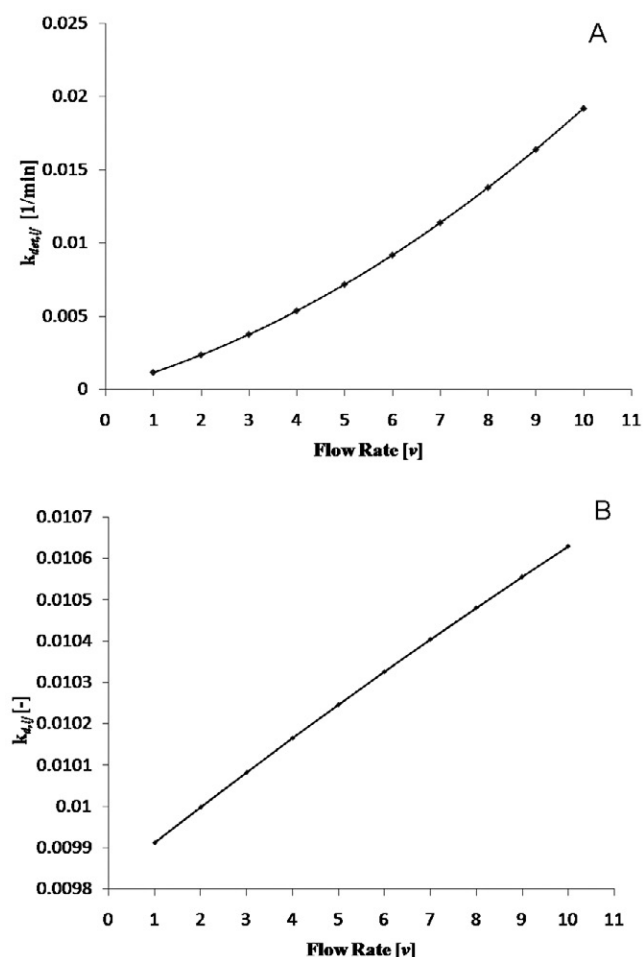


Fig. 7. (A) Detachment rate coefficient and (B) distribution coefficient shown as a function of flow rate.

pore network modeling and having attachment and detachment rate constants as a function of flow velocity.

Supplemental Material

Supplement 1 (Appendix A): Pore Network Modeling.
Supplement 2: video of rapid flow rate change on colloid remobilization during saturated flow in a micromodel.

Acknowledgments

This research was supported by the Fundamental Research Funds for the Central Universities (No. 35832015071). Dr. N.K. Karadimitriou is greatly acknowledged for his role in making the micromodels. Careful and comprehensive review by the Technical Editor Dr. Scott Bradford and two reviewers, which led to significant improvements of the manuscript, are greatly appreciated.

References

- Acharya, R., S. van der Zee, and A. Leijne. 2005. Transport modeling of nonlinearly adsorbing solutes in physically heterogeneous pore networks. *Water Resour. Res.* 41(2):W02020. doi:10.1029/2004WR003500
- Bergendahl, J., and D. Grasso. 1998. Colloid generation during batch leaching tests: Mechanics of disaggregation. *Colloids Surf. A Physicochem. Eng. Asp.* 135:193–205. doi:10.1016/S0927-7757(97)00248-3
- Bodla, K. K., J. Y. Murthy, and S. V. Garimella. 2010. Resistance network-based thermal conductivity model for metal foams. *Comput. Mater. Sci.* 50(2):622–632.
- Bradford, S.A., and M. Bettahar. 2006. Concentration dependent transport of colloids in saturated porous media. *J. Contam. Hydrol.* 82:99–117.
- Bradford, S.A., H.N. Kim, B.Z. Haznedaroglu, S. Torkzaban, and S.L. Walker. 2009. Coupled factors influencing concentration dependent colloid transport and retention in saturated porous media. *Environ. Sci. Technol.* 43:6996–7002.
- Bradford, S.A., J. Simunek, M. Bettahar, Y.F. Tadassa, M.T. van Genuchten, and S.R. Yates. 2005. Straining of colloids at textural interfaces. *Water Resour. Res.* 41. doi:10.1029/2004WR003675
- Bradford, S.A., J. Simunek, M. Bettahar, M.T. van Genuchten, and S.R. Yates. 2003. Modeling colloid attachment, straining, and exclusion in saturated porous media. *Environ. Sci. Technol.* 37:2242–2250. doi:10.1021/es025899u
- Bradford, S.A., and S. Torkzaban. 2008. Colloid transport and retention in unsaturated porous media: A review of interface-, collector-, and pore-scale processes and models. *Vadose Zone J.* 7:667–681. doi:10.2136/vzj2007.0092
- Bradford, S.A., S. Torkzaban, and J. Simunek. 2011. Modeling colloid transport and retention in saturated porous media under unfavorable attachment conditions. *Water Resour. Res.* 47. doi:10.1029/2011WR010812
- Bradford, S.A., and S. Torkzaban. 2013. Colloid interaction energies for physically and chemically heterogeneous porous media. *Langmuir* 29:3668–3676. doi:10.1021/la400229f
- Bradford, S.A., S. Torkzaban, F. Leij, J. Simunek, and M.T. van Genuchten. 2009. Modeling the coupled effects of pore space geometry and velocity on colloid transport and retention. *Water Resour. Res.* 45. doi:10.1029/2008WR007096
- Bradford, S.A., S. Torkzaban, and S.L. Walker. 2007. Coupling of physical and chemical mechanisms of colloid straining in saturated porous media. *Water Res.* 41:3012–3024. doi:10.1016/j.watres.2007.03.030
- Bradford, S.A., S.R. Yates, M. Bettahar, and J. Simunek. 2002. Physical factors affecting the transport and fate of colloids in saturated porous media. *Water Resour. Res.* 38(12). doi:10.1029/2002WR001340
- Burdick, G., N. Berman, and S. Beaudoin. 2001. Describing hydrodynamic particle removal from surfaces using the particle Reynolds number. *J. Nanopart. Res.* 3:453–467. doi:10.1023/A:1012593318108
- Burdick, G.M., N.S. Berman, and S.P. Beaudoin. 2005. Hydrodynamic particle removal from surfaces. *Thin Solid Films* 488:116–123.
- Chen, G., R.S. Bedi, Y.S. Yan, and S.L. Walker. 2010. Initial colloid deposition on bare and zeolite-coated stainless steel and aluminum: Influence of surface roughness. *Langmuir* 26:12605–12613. doi:10.1021/la101667t
- Cleaver, J.W., and B. Yates. 1973. Mechanism of detachment of colloid particles from a flat substrate in turbulent flow. *J. Colloid Interface Sci.* 44:464–474. doi:10.1016/0021-9797(73)90323-8
- Cushing, R.S., and D.F. Lawler. 1998. Depth filtration: Fundamental investigation through three-dimensional trajectory analysis. *Environ. Sci. Technol.* 32:3793–3801. doi:10.1021/es9707567
- Derjaguin, B.V., and L.D. Landau. 1941. Theory of the stability of strongly charged lyophobic sols and of the adhesion of strongly charged particles in solutions of electrolytes. *Acta Physicochim. URSS* 14:733–762.
- Du, Y., C. Shen, H. Zhang, and Y. Huang. 2013. Effects of flow velocity and nonionic surfactant on colloid straining in saturated porous media under unfavorable conditions. *Transp. Porous Media* 98. doi:10.1007/s11242-013-0140-3
- Gregory, J. 1981. Approximate expressions for retarded van der Waals interaction. *J. Colloid Interface Sci.* 83:138–145. doi:10.1016/0021-9797(81)90018-7
- Goldman, A.J., R.G. Cox, and H. Brenner. 1967. Slow viscous motion of a sphere parallel to a plane wall: I. Motion through a quiescent fluid. *Chem. Eng. Sci.* 22:637–651. doi:10.1016/0009-2509(67)80047-2
- Hock, E.M.V., S. Bhattacharjee, and M. Elimelech. 2003. Effect of membrane surface roughness on colloid-membrane DLVO interactions. *Langmuir* 19:4836–4847. doi:10.1021/la027083c
- Hoek, E.M.V., and G.K. Agarwal. 2006. Extended DLVO interactions between spherical particles and rough surfaces. *J. Colloid Interface Sci.* 298:50–58. doi:10.1016/j.jcis.2005.12.031
- Israelachvili, J.N. 1992. Intermolecular and surface forces. 2nd ed. Academic Press, London.
- Johnson, W.P., X. Li, and S. Assemi. 2007. Deposition and re-entrainment dynamics of microbes and non-biological colloids during non-perturbed transport in porous media in the presence of an energy barrier to deposition. *Adv. Water Resour.* 30:1432–1454. doi:10.1016/j.advwatres.2006.05.020
- Johnson, W.P., H. Ma, and E. Pazmino. 2011. Straining credibility: A general comment regarding common arguments used to infer straining as the mechanism of colloid retention in porous media. *Environ. Sci. Technol.* 45:3831–3832. doi:10.1021/es200868e
- Johnson, W.P., E. Pazmino, and H. Ma. 2010. Direct observations of colloid retention in granular media in the presence of energy barriers and pitfalls of inferring mechanisms from indirect observations. *Water Res.* 44:1158–1169. doi:10.1016/j.watres.2009.12.014
- Johnson, W.P., X. Li., and S. Assemi. 2007. Deposition and re-entrainment dynamics of microbes and non-biological colloids during non-perturbed transport in porous media in the presence of an energy barrier to deposition. *Adv. Water Resour.* 30:1432–1454.
- Johnson, W.P., and M. Tong. 2006. Simulated and experimental influence of hetero-domain size on colloid deposition efficiencies on overall like-charged surfaces. *Environ. Sci. Technol.* 40:5015–502. doi:10.1021/es060450c
- Karadimitriou, N.K., V. Joekar-Niasar, S.M. Hassanizadeh, P.J. Kleingeld, and L.J. Pyrak-Nolte. 2012. A new micro-model experimental approach for two-phase flow studies; comparison with a pore-network model. *Lab Chip* 12:3413–3418. doi:10.1039/c2lc40530j
- Karadimitriou, N.K. 2013. Two-phase flow experimental studies in micro-models. Ph.D thesis, Department of Earth Sciences, Utrecht University, the Netherlands.
- Kohne, J., S. Schluter, and H. Vogel. 2011. Predicting solute transport in structured soil using pore network models. *Vadose Zone J.* 10:1082–1096. doi:10.2136/vzj2010.0158
- Li, X., and W.P. Johnson. 2005. Nonmonotonic variations in deposition rate coefficients of microspheres in porous media under unfavorable deposition conditions. *Environ. Sci. Technol.* 39:1658–1665. doi:10.1021/es048963b
- Li, X., C.L. Lin, J.L. Miller, and W.P. Johnson. 2006. Role of grain-to-grain contacts on profiles of retained colloids in porous media in the presence of an energy barrier to deposition. *Environ. Sci. Technol.* 40:3769–3774. doi:10.1021/es052501w
- Morales, V.L., B. Gao, and T.S. Steenhuis. 2009. Grain surface-roughness effects on colloidal retention in the vadose zone. *Vadose Zone J.* 8:11–20. doi:10.2136/vzj2007.0171
- Norde, W., and J. Lyklema. 1989. Protein adsorption and bacterial adhesion to solid surfaces: A colloid chemical approach. *Colloids Surf.* 38:1–13. doi:10.1016/0166-6622(89)80138-6
- Nsir, K., and G. Schäfer. 2010. A pore-throat model based on grain-size distribution to quantify gravity-dominated dnapi instabilities in a water-saturated homogeneous porous medium. *Compt. Rendus Geosci.* 342(12):881–891.
- O'Neill, M.E. 1968. A sphere in contact with a plane wall in a slow linear shear flow. *Chem. Eng. Sci.* 23:1293–1298. doi:10.1016/0009-2509(68)89039-6
- Raouf, A., and S. Hassanizadeh. 2012. A new formulation for pore-network modeling of two-phase flow. *Water Resour. Res.* 48(1):W01514. doi:10.1029/2010WR010180

- Raoof, A., S. Hassanizadeh, and A. Leijnse. 2010. Upscaling transport of adsorbing solutes in porous media: Pore-network modeling. *Vadose Zone J.* 9:624–636. doi:10.2136/vzj2010.0026
- Raoof, A., H.M. Nick, S.M. Hassanizadeh, and C.J. Spiers. 2013. Pore Flow: A complex pore-network model for simulation of reactive transport in variably saturated porous media. *Comput. Geosci.* 61:160–174. doi:10.1016/j.cageo.2013.08.005
- Seetha, N., M.M. Kumar, S.M. Hassanizadeh, and A. Raoof. 2014. Virus-sized colloid transport in a single pore: Model development and sensitivity analysis. *J. Contam. Hydrol.* 164:163–180. doi:10.1016/j.jconhyd.2014.05.010
- Sharma, M.S., H. Chamoun, D.S.H. Sita Rama Sarma, and R.S. Schechter. 1992. Factors controlling the hydrodynamic detachment of particles from surfaces. *J. Colloid Interface Sci.* 149:121–134. doi:10.1016/0021-9797(92)90398-6
- Shellenberger, K., and B.E. Logan. 2002. Effect of molecular roughness of glass beads on colloidal and bacterial deposition. *Environ. Sci. Technol.* 36:184–189. Page: 10
- Shen, C., Y. Huang, B. Li, and Y. Jin. 2008. Effects of solution chemistry on straining of colloids in porous media under unfavorable conditions. *Water Resour. Res.* 44:W05419. doi:10.1029/2007WR006580
- Shen, C., F. Wang, B. Li, Y. Jin, L.-P. Wang, and Y. Huang. 2012. Application of DLVO energy map to evaluate interactions between spherical colloids and rough surfaces. *Langmuir* 28:14681–14692. doi:10.1021/la303163c
- Suresh, L., and J.Y. Walz. 1996. Effect of surface roughness on the interaction energy between a colloidal sphere and a flat plate. *J. Colloid Interface Sci.* 183:199–213. doi:10.1006/jcis.1996.0535
- Sze, A., D. Erickson, L. Ren, and D. Li. 2003. Zeta-potential measurement using the Smoluchowski equation and the slope of the current–time relationship in electro osmotic flow. *J. Colloid Interface Sci.* 261:402–410. doi:10.1016/S0021-9797(03)00142-5
- Torkzaban, S., S.A. Bradford, and S.L. Walker. 2007. Resolving the coupled effects of hydrodynamics and DLVO forces on colloid attachment to porous media. *Langmuir* 23:9652–9660. doi:10.1021/la700995e
- Torkzaban, S., H.N. Kim, J. Simunek, and S.A. Bradford. 2010. Hysteresis of colloid retention and release in saturated porous media during transients in solution chemistry. *Environ. Sci. Technol.* 44:1662–1669.
- Varloteaux, C., S. Bekri, and P.M. Adler. 2012. Pore network modelling to determine the transport properties in presence of a reactive fluid: From pore to reservoir scale. *Adv. Water Resour.* 53:87–100.
- Verwey, E.J.W., and J.T.G. Overbeek. 1948. *Theory of the stability of lyophobic colloids.* Elsevier, Amsterdam.
- Weisbrod, N., O. Dahan, and E.M. Adar. 2002. Particle transport in unsaturated fractured chalk under arid conditions. *J. Contam. Hydrol.* 56:117–136. doi:10.1016/S0169-7722(01)00199-1
- Xu, S., B. Gao, and J.E. Saiers. 2006. Straining of colloidal particles in saturated porous media. *Water Resour. Res.* 42. doi:10.1029/2006WR004948
- Xu, S., Q. Liao, and J.E. Saiers. 2008. Straining of non-spherical colloids in saturated porous media. *Environ. Sci. Technol.* 42:771–778. doi:10.1021/es071328w
- Yao, K.M., M.T. Habibian, and C.R. O'Melia. 1971. *Water and wastewater filtration: Concepts and applications.* Environ. Sci. Technol. 5:1105–1112. doi:10.1021/es60058a005
- Zhang, Q.L., N.K. Karadimitriou, S.M. Hassanizadeh, P.J. Kleingeld, and A. Imhof. 2013. Study of Colloids Transport during Two-Phase Flow using a Novel Polydimethylsiloxane Micro-model. *J. Colloid Interface Sci.* 401:141–147. doi:10.1016/j.jcis.2013.02.041